



Photoluminescence properties of Tb³⁺ doped lithium aluminoborate phosphor, LiAlB₂O₅:Tb³⁺

R. S. Palasagar¹, R.P. Sonekar^{2*} and S.K.Omanwar¹

¹Department of Physics, SGB Amravati University, Amravati – 444 602 (M.S.) India,

²Department of Physics G.S. College, Khamgaon – 444 303, Dist.-Buldana (M.S.) India.

Abstract

A novel green phosphor, Tb³⁺ doped LiAlB₂O₅ (LABO) has been synthesized by the solution combustion method of corresponding metal nitrates (oxidizer) and urea (fuel) at furnace temperature as low as 550 °C. The phase purity and morphology of LABO samples have been characterized by powder X-ray diffraction (XRD) and scanning electron microscopy (SEM), respectively. Photoluminescence spectra of the phosphor at room temperature exhibited emissions at 489, 549 and 586 nm, which were assigned to the ⁵D₄→⁷F₆, ⁵D₄→⁷F₅ and ⁵D₄→⁷F₄ transitions of Tb³⁺ respectively. Among them, the green emission at 549 nm (⁵D₄→⁷F₅) was dominant. For the 549 nm emission, the excitation spectrum has strong excitation peak locates at 229 nm. The dependence of the emission intensity on the Tb³⁺ concentration for the Li_(1-x)AlB₂O₅: xTb³⁺ (0.01 ≤ x ≤ 0.03) was studied. It was observed that 0.025 mol % of doping concentration of Tb³⁺ ions in prepared phosphor was optimum. Concentration quenching of Tb³⁺ emission in LABO has been studied.

Keywords: Green phosphors; LiAlB₂O₅:Tb³⁺; combustion method; Photoluminescence.

PACS Code:78.55-m

1.0 Introduction

In recent years, the new lighting and display technology such as light-emitting diodes (LEDs), plasma display panels (PDPs), and field emission displays (FEDs) have been proposed or developed in industry, which result in great interest in searching novel phosphors for these new applications [1-6]. Tb³⁺ doped materials have been widely used as green emitting phosphor due to its intense ⁵D₄→⁷F₅ emission in the green spectral region. Previous studies have shown that Tb³⁺ doped phosphates, aluminates or borates exhibit relatively strong absorption in the NUV region and intense green emission with good color purity [7-10]. The Tb³⁺ is a kind of important activator with sharp 4f→4f emission peak in the green region of visible spectrum, specially generating green emission with good color purity centered at around 543 nm, corresponding to the ⁵D₄→⁷F₅ transitions [11-12]. However, the absorption transition of Tb³⁺ is difficult to pump owing to the absolutely forbidden 4f→4f electric dipole transitions. In case of Tb³⁺ ion, the absorption is usually due to allowed f → d transition from excited state of 4f⁷ 5d¹ configuration, the electron loses energy to lattice and blue region while ⁵D₄→⁷F_j emission is pre-dominantly green. At lower concentrations, blue emission is observed; but at higher concentration, there is an energy transfer between Tb³⁺ ions, e.g. the cross relaxation Tb³⁺ (⁵D₃) + Tb³⁺ (⁷F_j) → Tb³⁺ (⁵D₄) + Tb³⁺ (⁷F₀), due to which the blue emission gets quenched increasing the green emission at the same time. Tb³⁺ emission may

be efficiently sensitized by transfer from sensitizer to 4fⁿ levels. The energy transfer is introduced between the broad band excitation of 4f→5d transition ions and the sharp line emission of 4f→4f transition ions [13]. In this study, LiAlB₂O₅:Tb³⁺ phosphors were prepared by conventional solid state reaction method. The phase and surface morphology of synthesized materials were investigated using the XRD and SEM. After synthesis and characterization of the phosphors, the photoluminescence properties of the synthesized phosphors were studied using a spectrofluorometer at room temperature. Further the dependence of the emission intensity on the Tb³⁺ concentration for the Li_(1-x)AlB₂O₅: xTb³⁺ (0.01 ≤ x ≤ 0.03) was studied in detail.

2.0 Materials and method

The powder samples of Tb³⁺ activated LABO phosphor were prepared by a solution combustion technique. In our previous work, many borate materials were successfully synthesized using this technique [14-18]. High purity starting materials, Li(NO₃)₂ (A.R.), Al(NO₃)₃.9H₂O (A.R.), Tb(NO₃)₃ (high purity 99.9%), H₃BO₃ (A.R.), CO(NH₂)₂ (A.R.) were used for the phosphor preparation. The stoichiometric amounts of the ingredients were thoroughly mixed in an Agate Mortar with adding little amount of double distilled water. The material then transferred into china basin and heated on heating menthol at about 70°C so as to obtained clear solution. The solution was then introduced into a pre-heated muffle furnace maintained at temperature 550 °C for combustion. The solution boils; foams and

ignites to burn with flame which gave a voluminous, foamy powder. Following the combustion, the resulting foamy samples were crushed to obtain fine particles and then annealed in a slightly reducing atmosphere provided by burning charcoal at temperature 750 °C for 2 hr and suddenly cooled to room temperature.

The prepared materials were characterized by powder XRD. Powder X-ray diffraction measurements were taken on Rigaku Miniflex II X-ray Diffractometer and compared with the ICDD file. PL & PLE measurements at room temperature were performed on Hitachi F-7000 spectrofluorometer with spectral resolution of 2.5 nm.

3.0 Results and discussion

3.1. X-ray diffraction pattern

The X-ray diffraction (XRD) technique was used to identify the phase composition, structure and their crystallinity. Fig. 1 shows the XRD pattern of $\text{LiAlB}_2\text{O}_5:\text{Tb}^{3+}$ phosphor. The XRD pattern of the as prepared phosphor powder shows good agreement with standard ICDD File. The ionic radius of Tb^{3+} (0.923 Å) is larger than Li^+ (0.76 Å) and Al^{3+} (0.535 Å); Tb^{3+} ions may enter into the host lattice to substitute Al^{3+} or Li^+ or locate on the surface of the crystal. It would have greater tendency to occupy lithium as compared to aluminum sites.

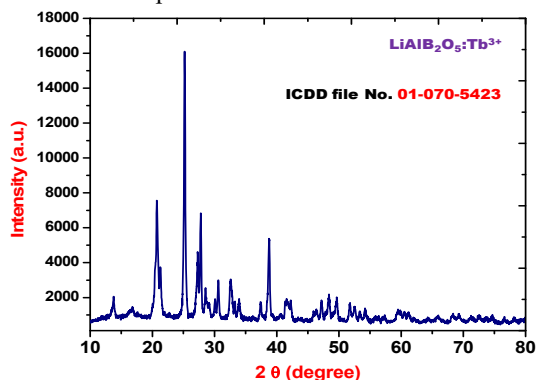


Fig. 1: X-ray powder diffraction pattern of $\text{LiAlB}_2\text{O}_5:\text{Tb}^{3+}$ phosphor.

3.2. SEM images of phosphor powders

The SEM photographs of $\text{LiAlB}_2\text{O}_5:\text{Tb}^{3+}$ powder synthesized by using solution combustion method is shown in Fig. 2. The morphology of particles are crystalline and mostly with some random shaped crystals. The mean diameter of the particle is approximately 1 to 2 μm; the particles grow together and form larger aggregates, due to high temperature synthesis processes. It is clear that the particles are tightly bonded together to form large agglomerates.

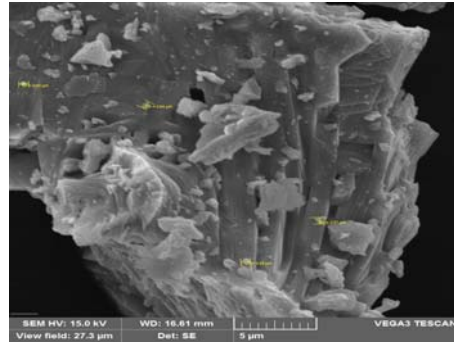


Fig 2: SEM image of $\text{LiAlB}_2\text{O}_5:\text{Tb}^{3+}$ phosphor.

3.3. Photoluminescence study

Fig. 3 gives the excitation and emission spectra of Tb^{3+} doped LABO phosphor. The excitation spectrum shows broad band ranging from 200 to 350 nm with intense peak around 229 nm. The as prepared phosphor compositions exhibits emission in the blue-green region as shown in Fig. 4(A). The emission bands show a splitting pattern, such as $^5\text{D}_4 \rightarrow ^7\text{F}_5$ transition of Tb^{3+} (543 and 549 nm) **Error! Bookmark not defined.** The intensity of peak at 546 nm is more than that of peak at 549 nm. $\text{LiAlB}_2\text{O}_5:\text{Tb}^{3+}$ powders exhibited several emission lines peaking at 489, 543, 549, 586 and 594 nm, which were assigned to the $^5\text{D}_4 \rightarrow ^7\text{F}_j$ ($J=6, 5, 4, 3, 2$) transitions of Tb^{3+} , respectively. Among them, the green emission at 543 nm ($^5\text{D}_4 \rightarrow ^7\text{F}_5$) was dominant.

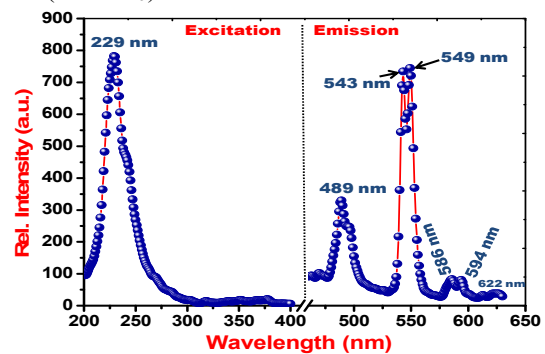


Fig. 3: Representative PL excitation and emission spectra of $\text{LiAlB}_2\text{O}_5:0.025\text{Tb}^{3+}$ phosphor.

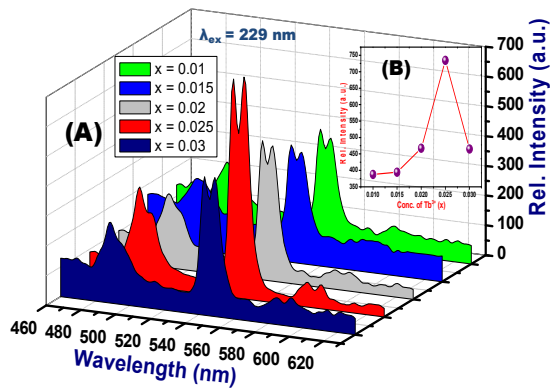


Fig. 4: (A) Dependence of the PL intensities of $\text{Li}_{(1-x)}\text{AlB}_2\text{O}_5: x\text{Tb}^{3+}$ ($0.01 \leq x \leq 0.03$) at $\lambda_{\text{ex}}=229$ nm at different Tb^{3+} concentrations. (B) The top inset shows the influence of the concentration on the emission intensity of $\text{Li}_{(1-x)}\text{AlB}_2\text{O}_5: x\text{Tb}^{3+}$ ($0.01 \leq x \leq 0.03$) phosphor.

The cross-relaxation of adjacent Tb^{3+} ions led to the main emission peaks locate at 489 and 543 nm under excitation of 229 nm. Local crystal field symmetry around the Tb^{3+} cations can have a significant effect on electric dipole transitions. However, when the crystal size is decreased, surface defects decrease the local symmetry around the Tb^{3+} cations, increasing the intensity of the green emission.

3.3.1. Concentration quenching mechanism of Tb^{3+} in $\text{Li}_{(0.975)}\text{AlB}_2\text{O}_5:0.025\text{Tb}^{3+}$

In order to optimize the green emission of Tb^{3+} , the concentration dependent emission intensity of $\text{Li}_{(1-x)}\text{AlB}_2\text{O}_5: x\text{Tb}^{3+}$ ($x=0.01, 0.015, 0.02, 0.025, 0.03$) was studied. Fig. 4(B) shows that the dependence of the emission intensities of $\text{Li}_{(1-x)}\text{AlB}_2\text{O}_5: x\text{Tb}^{3+}$ ($x=0.01, 0.015, 0.02, 0.025, 0.03$) phosphors under 229 nm excitation. However, the emission intensity of Tb^{3+} initially increases, then reaches a maximum at $x=0.025$, and finally decreases. The critical transfer distance (R_c) is the critical separation between donor and acceptor, at which the non radiative rate equals that of the internal single ion relaxation. It is approximately equal to twice the radius of a sphere with this volume [19]:

$$R_c = 2 \left(\frac{3V}{4\pi x_c N} \right)^{1/3} \quad (1)$$

Where x_c is the critical concentration, N the number of cation in the unit cell and V the volume of the unit cell ($N=6, V=306.12 \text{ \AA}^3$ for LABO). R_c is calculated to be about 12.49 \AA . The resonant energy transfer mechanism consists of two types: exchange or multipolar interaction. For the exchange interaction, R_c is generally shorter than $0.3\text{--}0.4$ nm. Therefore, the energy transfer mechanism in LABO: Tb^{3+} is considered as a multipolar interaction. The quenching mechanism is associated with the interaction between

the one excited ion and another, and the emission intensity per activator ion follows the equation [20]:

$$I/x = K[1 + \beta(x)^Q/3]^{-1} \quad (2)$$

where x is the activator concentration; $Q=6, 8, 10$ for dipole-dipole (d-d), dipole-quadrupole (d-p), quadrupole-quadrupole (q-q) interactions, respectively; and K and β are the constants for the same excitation conditions in a given host crystal. The critical concentration of Tb^{3+} has been determined to be 0.025 mole. The plot of $\lg(I/x)$ as function of $\lg(x)$ in LABO: Tb^{3+} phosphor is obtained by using Dexter's theory [21], and shown in Fig. 5. It represents that the dependence of $\log(I/x)$ on $\log(x)$ is linear and the slope is -1.733 . The value of Q was calculated as 5.2 (close to 6). This suggests that the electric d-d interaction is responsible for the concentration quenching mechanism of Tb^{3+} emission in LABO: Tb^{3+} phosphor.

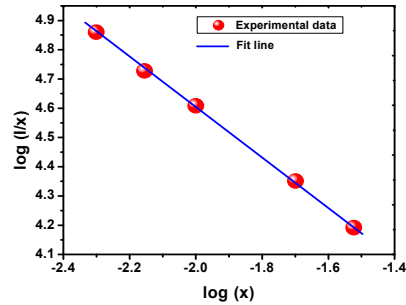


Fig. 5: Plot of $\log(I/x)$ as function of $\log(x)$ in $\text{Li}_{(1-x)}\text{AlB}_2\text{O}_5: x\text{Tb}^{3+}$ phosphor ($x=0.01, 0.015, 0.02, 0.025, 0.03$) ($\lambda_{\text{ex}}=229$ nm).

The CIE chromaticity coordinates for $\text{Li}_{(0.975)}\text{AlB}_2\text{O}_5:0.025\text{Tb}^{3+}$ were calculated from the PL spectra under 229 nm excitation and marked with a white star in the CIE 1931 chromaticity diagram in Fig. 6. The chromaticity coordinates (x, y) of this phosphor are $(0.2944, 0.6988)$, respectively, which indicates that the emission color of the as prepared phosphors is located in the green region.

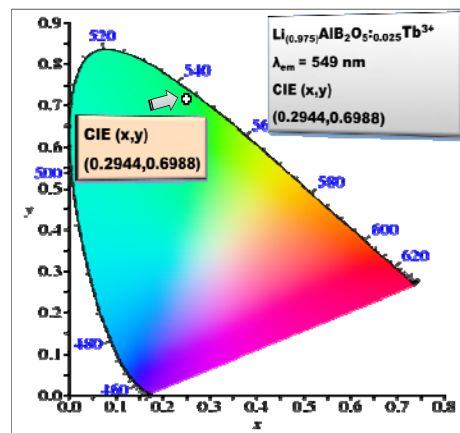




Fig. 6: Chromaticity coordinates of $\text{Li}_{(0.975)}\text{AlB}_2\text{O}_5:0.025\text{Tb}^{3+}$ phosphor in the CIE 1931 chromaticity diagram.

4. Conclusions

The phosphor $\text{LiAlB}_2\text{O}_5:\text{Tb}^{3+}$ has been successfully synthesized by using a simple, time saving and cost effective solution combustion technique. The as synthesized phosphor shows mainly two emission bands located at blue (489 nm) and green band (544 nm) corresponding to the $^5\text{D}_4 \rightarrow ^7\text{F}_5$ transition spectra region originated from the transition of Tb^{3+} ions. It is found that 0.025 mol% doping concentration of Tb^{3+} ions in LABO phosphor is optimum in the host lattice. LABO: Tb^{3+} phosphor can be used for generating green light under UV radiation.

Acknowledgement

One of the authors (RSP) wishes to thank The Chairman, FIST project, SGB Amravati University, Amravati (MS) for providing powder X-ray Diffraction facility for this work.

References:

1. Z. Xiang, X. Yang, B. Zhou, X. Liu, Q. Wen, X. Jin, S. Xiao, *Physica B*, 431 (2013) 132–136.
2. D.Y. Wang, Y.C. Chen, C.H. Huang, B.M. Cheng, T.M. Chen, *J. Mater. Chem.*, 22 (2012) 9957.
3. Y. Deng, S. Yi, J. Huang, W. Zhao, J. Xian, *Physica B*, 433 (2014) 133–137.
4. S. Ye, F. Xiao, Y.X. Pan, Y.Y. Ma, Q.Y. Zhang, *Mater. Sci. Eng. R*, 71 (2010) 1–34.
5. C.V. Devi, G. Phaomei, N. Yaiphaba, N.R. Singh, *J. Alloys Compd.*, 583 (2014) 259–266.
6. Z. Xia, Y. Zhang, M.S. Molokeev, V.V. Atuchin, Y. Luo, *Sci. Rep.*, 3 (2013) 3310-1-7.
7. Z. Liang, J. Zhang, J. Sun, X. Li, L. Cheng, H. Zhong, S. Fu, Y. Tian, B. Chen, *Physica B*, 412 (2013) 36.
8. Y. S. Kawashima, C. F. Gugliotti, M. Yee, S. H. Tatum, J. C. R. Mittani, *Radiat. Phys. Chem.*, 95 (2014) 91.
9. Q. Guo, L. Liao, Z. Xia, *J. Lumin.*, 145 (2014) 65.
10. H. Lai, Y. Du, M. Zhao, K. Sun, L. Yang, *Mater. Sci. Eng. B.*, 179 (2014) 66.
11. H. L. Yu, X. Xu, X. H. Xu, T. M. Jiang, P. H. Yang, Q. Jiao, D. C. Zhou, J. B. Qiu, *Opt. Commun.*, 317 (2014) 78.
12. G. G. Zhang, J. Wang, Y. Chen, Q. Su, *Opt. Lett.*, 35 (2010) 2382.
13. Z. G. Xia, J. Q. Zhuang, H. K. Liu, L. B. Liao, *J. Phys. D: Appl. Phys.*, 45 (2012) 015302.
14. R. S. Palaspagar, A. B. Gawande, R. P. Sonekar, S. K. Omanwar, *J. Lumin.*, 154 (2014) 58.
15. R. S. Palaspagar, A. B. Gawande, R. P. Sonekar, S. K. Omanwar, *Mater. Res. Bull.*, 72 (2015) 215.
16. R. S. Palaspagar, R. P. Sonekar, S. K. Omanwar, in *AIP Conf.*, 807 (2013).
17. R. S. Palaspagar, A. B. Gawande, R. P. Sonekar, S. K. Omanwar, *J. Chinese Adv. Mater. Soc.*, 1 (2015) 176.
18. R. S. Palaspagar, A. B. Gawande, R. P. Sonekar, S. K. Omanwar, *Int. J. light & electron opt.*, 126 (2015) 5030.
19. G. Blasse, *Philips Res. Rep.*, 24 (1969) 131.
20. G. Zhu, Y. Wang, Z. Ci, B. Liu, Y. Shi, S. Xin, *J. Lumin.*, 132 (2012) 531.
21. D.L. Dexter, J.H. Schulman, *J. Chem. Phys.*, 22 (1954) 1063.